Fragmentation of Doubly-Protonated Pro-His-Xaa Tripeptides: Formation of b_2^{2+} Ions

Michaela Knapp-Mohammady,[b] Alex B. Young,[a] Béla Paizs,[b] and Alex G. Harrison[a]

[a] Department of Chemistry, University of Toronto, Toronto, Canada
[b] Department of Molecular Biophysics, German Cancer Research Center (DKFZ), Heidelberg, Germany

When ionized by electrospray from acidic solutions, the tripeptides Pro-His-Xaa (Xaa = Gly, Ala, Leu) form abundant doubly-protonated ions, $[M + 2H]^{2+}$. Collision-induced dissociation (CID) of these doubly-protonated species results, in part, in formation of b_2^{2+} ions, which fragment further by loss of CO to form a_2^{2+} ions; the latter fragment by loss of CO to form the Pro and His iminium [immonium is commonly used in peptide MS work] ions. Although larger doubly-charged b ions are known, this represents the first detailed study of b_2^{2+} ions in CID of small doubly protonated peptides. The most abundant CID products of the studied doubly-protonated peptides arise mainly in charge separation involving two primary fragmentation channels, formation of the b_2/y_1 pair and formation of the a_1/y_2 pair. Combined molecular dynamics and density functional theory calculations are used to gain insight into the structures and fragmentation pathways of doubly-protonated Pro-His-Gly including the energetics of potential protonation sites, backbone cleavages, post-cleavage charge-separation reactions and the isomeric structures of b_2^{2+} ions. Three possible structures are considered for the b_2^{2+} ions: the oxazolone, diketopiperazine, and fused ring isomers. The last is formed by cleavage of the His-Gly amide bond on a pathway that is initiated by nucleophilic attack of one of the His side-chain imidazole nitrogens. Our calculations indicate the b_2^{2+} ion population is dominated by the oxazolone and/or fused ring isomers.   (J Am Soc Mass Spectrom 2009, 20, 2135–2143) © 2009 American Society for Mass Spectrometry

With the introduction of the soft ionization techniques of electrospray ionization (ESI) [1–3] and matrix-assisted laser desorption ionization (MALDI) [4, 5], tandem mass spectrometry [6, 7] of protonated or multiply-protonated peptides has become the method of choice for identifying the amino acid sequence of peptides. As a result of many studies, the main fragmentation channels of singly-protonated peptides have been established, and considerable progress has been made in understanding, in detail, the mechanistic aspects of the fragmentation reactions; these studies have been the subject of several recent reviews [8–13].

In the field of proteomics, one frequently studies the fragmentation of tryptic peptides, and it has been found that more sequence information is often obtained by studying the fragmentation of multiply-charged precursors. Early mechanistic studies were limited to the basic fragmentation patterns of doubly-protonated peptides [14–17]; more recently the factors that control the fragmentation modes have seen more analysis by statistical characterization of tandem mass spectral databases [18,

19]. A kinetic model of the low-energy fragmentation of multiply-protonated peptides also has shown promise [20].

Very recently, Bleiholder et al. [21] investigated the structure and reactivity of doubly-protonated G_5R by studying CID in an ion trap instrument and detailed scans of the corresponding potential energy surface. These studies indicate that fragmenting species form doubly-charged post-reaction complexes (Scheme 1), which are stabilized by strong H-bonds via proton bridges. These complexes will be referred to as doubly-protonated dimers (DPD). Two major inter-converting forms of the DPDs exist: a symmetrically charged s-DPD, where both monomers carry an extra proton (ion/ion complex), and the asymmetrically charged as-DPD, where one of the fragments is doubly-protonated and the other is neutral (ion/dipole complex). The s-DPD dissociates in a charge separation process during which the dissociating species must overcome a charge separation barrier. On the other hand, the as-DPD dissociates in an endothermic but barrier-less process (in other words no barrier exists for the reverse process). It is worth noting here that the dissociation products formed from s-DPD (two singly protonated species) are energetically likely to be more favored than the products formed from as-DPD (a doubly-charged and a neutral species). This is because the secondary proton affinities (PAs) of molecules formed as peptide
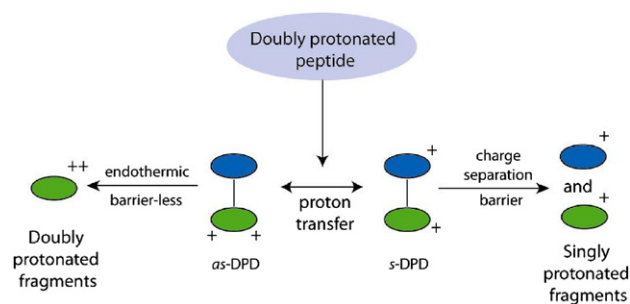
Scheme 1. Fate of doubly-charged post-reaction complexes (DPDs, doubly-protonated dimers) formed upon fragmentation of doubly-protonated peptides.

fragments are usually much lower than the primary PAs of these species. The *as*-DPD dissociation channel becomes competitive only if a significant charge separation barrier is to be crossed during dissociation of the *s*-DPD.

We have observed that tripeptides with the sequence Pro-His-Xaa form abundant doubly-protonated species, $[M + 2H]^{2+}$. This affords the opportunity to study, in detail, the fragmentation reactions of relatively simple doubly-protonated species. A significant fragmentation channel on collisional activation was found to involve loss of the C-terminal residue as a neutral amino acid to form b_2^{2+} ions. Large doubly-charged *b* ions are frequently observed (see, for example Haselmann et al. [22], and there is a brief mention [23] of a doubly-charged b_2 ion produced by CID of doubly-protonated substance P (an eleven residue peptide). However, this is, to our knowledge, the first observation of a b_2^{2+} ion upon CID of small doubly-charged peptide precursors. In addition, it is the first detailed study of the formation and fragmentation modes of such small doubly-charged b_2 ions. It is worth noting here that doubly-charged a_3^{2+} and a_2^{2+} ions of GGG were recently observed [24] in CID of $[La(GGG)(CH_3CN)_2]^{3+}$.

Fragmentation of histidine containing peptides attracted some attention [11, 25, 26] in the past, still many aspects of the related dissociation chemistry are not clarified yet. The histidine side chain has a relatively high proton affinity [27, 28] and, therefore, it is likely to be protonated if the number of added protons is higher than the number of arginines and lysines present in the peptide ion under study. The side-chain imidazole group can initiate cleavage of the C-terminal adjacent amide bond to form alternative non-oxazolone *b* ions. This reaction was studied by Wysocki and coworkers [11] using various experimental techniques, while O'Hair and coworkers [26] showed that the alternative *b* ion is indeed a stable structure using quantum chemical calculations. A plausible mechanism that explains the observed experimental behavior includes proton transfer to the C-terminal adjacent amide N and subsequent nucleophilic attack by the His side-chain on the carbon center of the protonated amide bond [13]. O'Hair in another study [25] demonstrated that CID of

the b_2 ion of Gly-His and His-Gly produces the same fragmentation pattern that parallels that of the diketopiperazine derivative *cyclo*-GH.

The results of our studies on the fragmentation patterns of doubly-protonated Pro-His-Xaa tripeptides (Xaa = Gly, Ala, and Leu) are presented in the following along with modeling data on the structure and fragmentation pathways of doubly-protonated Pro-His-Gly. Calculations were performed for the His-side-chain initiated, diketopiperazine, and b_n-y_m (oxazolone) cleavages of the His-Gly amide bond, which lead to various b_2^{2+} ion isomers. The post-cleavage phase of fragmentation is analyzed by considering the structure and dissociation energetics of the DPDs formed on the b_n-y_m (oxazolone) pathway.

Experimental

All experimental work was carried out using an electrospray/quadrupole/time-of-flight (QqTOF) mass spectrometer (QStar; MDS SCIEX, Concord, Canada). MS/MS experiments were carried out in the usual fashion by mass-selecting the ions of interest with the mass analyzer Q with CID in the quadrupole collision cell q and mass analysis of the ionic products with the time-of-flight analyzer. In the study of fragment ions (pseudo-MS[3] experiments), CID in the interface region produced fragment ions with those of interest being selected by the quadrupole mass analyzer Q for fragmentation and analysis in the usual manner. The cone voltage was adjusted to give the best yield of the fragment ion of interest; typically a cone voltage of 50–60 V was optimal.

The peptide samples, at micromolar concentrations, were introduced into the electrospray source in 1:1 CH_3OH:2% aqueous formic acid from a syringe pump at a flow rate of 80 $\mu L\ min^{-1}$. The electrospray needle was held at 5100 V. In the absence of formic acid the signals for the doubly-protonated peptides were very weak. Nitrogen was used as nebulizing and drying gas and as collision gas in the quadrupole collision cell. Doubly-charged ion signals were identified by the half-mass separation of the isotopic peaks.

All peptide samples (Pro-His-Gly, Pro-His-Ala, Pro-His-Leu, and Leu-His-Leu) were obtained from Bachem Biosciences (King of Prussia, PA) and showed no impurities in their mass spectra. Consequently, they were used as received.

Calculations

Our conformational search engine [29–34] devised specifically to deal with protonated peptides was used to scan the potential energy surface (PES) of [Pro-His-Gly + 2H]$^{2+}$. These calculations began with molecular dynamics (MD) simulations on various forms of [Pro-His-Gly + 2H]$^{2+}$ using the InsightII program (Biosym Technologies, San Diego, CA, USA), in conjunction with the AMBER force field [35] modified by us to allow

scans on amide nitrogen protonated species, oxazolone terminated structures, and b_n-y_m type [31, 36] transition structures (TS). During the MD simulations, structures were regularly saved for further refinement by full geometry-optimization using the same force field. In the next stage of the calculations, these structures were analyzed by our own conformer-family search program. This program groups optimized structures into families based on the similarity of the most important characteristic torsion angles. The most stable species in these families were then fully optimized at the HF/3-21G, B3LYP/6-31G(d) and the B3LYP/6-31+G(d,p) levels. The conformer families were regenerated at each theoretical level.

Having scanned the PES, transition structures corresponding to the various fragmentation pathways of [Pro-His-Gly + 2H]$^{2+}$ were then sought using calculations at the B3LYP/6-31G(d) and B3LYP/6-31+G(d,p) levels of theory. The resulting TSs were checked using intrinsic reaction coordinate (IRC) calculations to unambiguously define which minima are connected by the TS investigated. Post-reaction complexes on the b_2-y_1 pathway were characterized at the B3LYP/6-31G(d) and B3LYP/6-31+G(d,p) levels of theory in a manner similar to that used for the various [Pro-His-Gly + 2H]$^{2+}$ structures. Relative energies were calculated by using the B3LYP/6-31+G(d,p) total energies and zero-point energy corrections (ZPE) determined at the B3LYP/6-31G(d) level. Entropies were calculated using the rigid-rotor harmonic oscillator (RRHO) approximation. The Gaussian [37] suite of programs was used for all ab initio and DFT calculations.

Results and Discussion

CID of Doubly-Protonated PHG, PHA, PHL, and LHL

With the acidic solvent the doubly-protonated ion signals [M + 2H]$^{2+}$ were usually of at least equal intensity as the [M + H]$^{+}$ ion signals. Good quality CID mass spectra were obtained at offset voltages of the quadrupole collision cell of 12–15 V, corresponding, for a doubly-charged ion, to collision energies in the laboratory frame of 24–30 eV.

Figure 1 to Figure 2 present the CID mass spectra for the [M + 2H]$^{2+}$ ions of Pro-His-Gly, Pro-His-Ala, and Pro-His-Leu. Many of the fragments can be assigned as primary dissociation products originating from cleavages of either the Pro-His or His-Xaa amide bonds. These include singly charged fragments like b_2, y_2, y_1, and a_1 (Pro iminium ion, I_P). All spectra show ion signals corresponding to the doubly-charged b_2^{2+} and a_2^{2+} at m/z 118 and m/z 104, respectively. (The b_2^{2+} ion has an additional proton compared to the b_2^{+} ion and, properly, should be identified as b_2H^{2+}. For simplicity, it appears to be the custom not to specify the additional proton.) In the same vein, it should be noted that the b_2^{2+} ion reported briefly by Quin and Yuan [23] con-
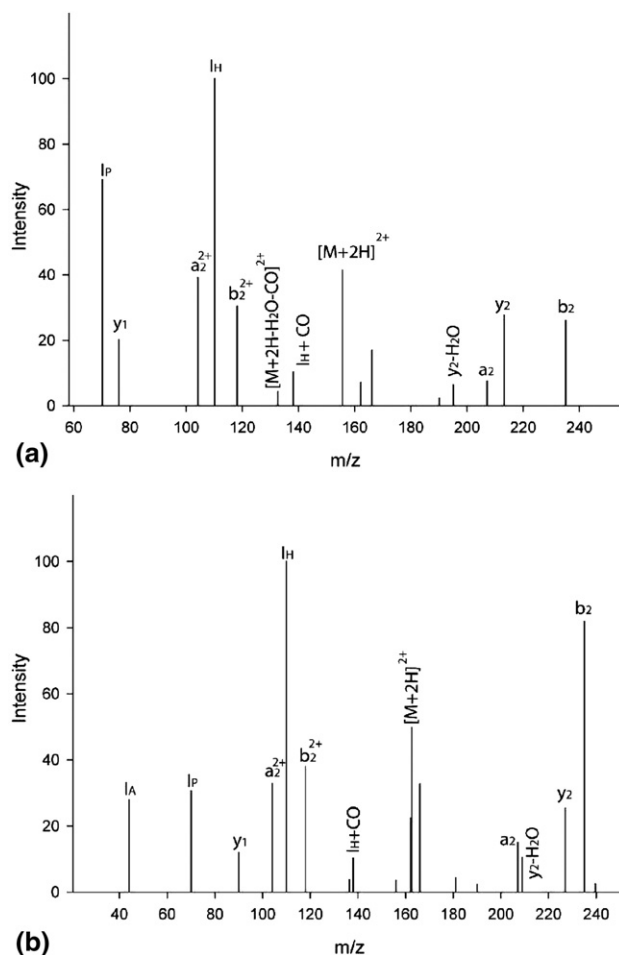

Figure 1. CID spectra of the [M + 2H]$^{2+}$ ions of (a) Pro-His-Gly and (b) Pro-His-Ala. I_x denotes the iminium ion of amino acid X.

tains a basic Arg residue as well as a proline residue. In addition, both Pro-His-Gly and Pro-His-Ala show weak ion signals corresponding to the a_3^{2+} ion (loss of H$_2$O + CO) at m/z 132.6 and m/z 139.6 (not labeled), respectively. In contrast to the tripeptides with Pro in the N-terminal position, doubly-protonated Leu-His-Leu does not show (Figure 2b) formation of doubly-charged fragment ions upon collisional activation. This indicates that the N-terminal proline residue plays an important role in formation of the observed doubly-charged fragments and its nitrogen is likely to be protonated in these ions.

The fragmentation pathways of doubly-protonated Pro-His-Gly, Pro-His-Ala, and Pro-His-Leu are summarized in Scheme 2. Cleavage of the His-Xaa amide bond leads to the primary b_2, y_1, and b_2^{2+} fragments. Pseudo-MS^3 studies (data not presented) of the b_2^{2+} ion showed three fragments, the a_2^{2+} ion and the two iminium ions m/z 70 (Pro, I_P) and m/z 110 (His, I_H), the latter two in approximately equal abundance. These results are consistent with initial loss of CO to form the a_2^{2+} ion followed by charge separation to form the two iminium ions and neutral CO (Scheme 2). A similar fragmentation pattern has been observed for the disso-
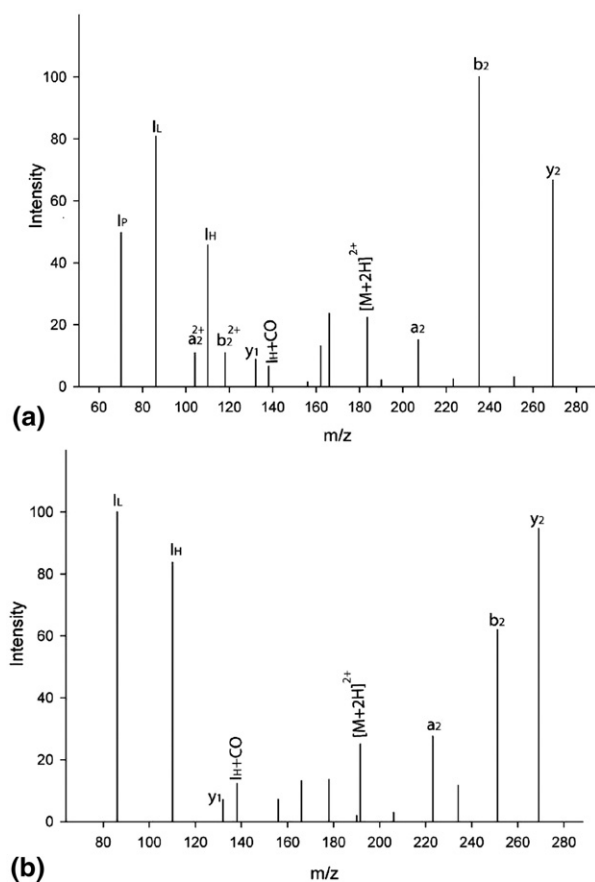
Figure 2. CID spectra of the [M + 2H]$^{2+}$ ions of (**a**) Pro-His-Leu and (**b**) Leu-His-Leu. I$_x$ denotes the iminium ion of amino acid X.

ciation of singly charged a_2 ions [38]. Pseudo-MS^3 experiments (data not shown) indicate that the singly charged b_2 fragments further to form a_2, the His and Pro iminium ions (I$_H$ and I$_P$) and fragments at m/z 162 and 166 (Scheme 2), respectively.

Cleavage of the Pro-His amide bond leads to y_2 and the iminium ion of Pro (Scheme 2), no doubly-charged dissociation product is observed here. The I$_P$/y_2 and the b_2/y_1 ion pairs are formed in apparent charge separation reactions (e.g., from s-DPDs of Scheme 1) that produce at higher than the precursor m/z, the b_2 and y_2 singly-charged ions. If, as proposed, the b_2 ion arises by charge separation fragmentation of [M + 2H]$^{2+}$, one would expect corresponding ion signals for the y_1 ion and its fragmentation product, the appropriate iminium ion [39, 40]. In each spectrum the appropriate y_1 ion is observed as well as the iminium ion formed by loss of H$_2$O + CO from y_1. (The iminium ion signal (m/z 30) derived from Pro-His-Gly was very weak, possibly because of discrimination against low-mass products in the QqTOF instrument.) Further, one would expect that summed signals for the b_2 ion plus fragments derived therefrom should equal the signal for the y_1 ion plus fragments derived therefrom. Due to the unknown, but possibly substantial, further fragmentation of b_2 it is not possible to compare quantitatively the relative ion sig-

nals although it does appear that the b_2 ion plus fragments are more intense than the y_1 ion plus fragments. The reasons for this phenomenon are not clear. Similarly, formation of the y_2 ion by charge separation should be accompanied by formation of the proline iminium ion (m/z 70) for the Pro-His-Xaa peptides and the leucine iminium ion (m/z 86) for the Leu-His-Leu tripeptide. This appears to be roughly true, although, again, quantitative analysis is difficult because of further fragmentation.

Comparing the CID spectra in Figures 1 and 2, one easily observes that the weight of the doubly-charged b_2^{2+} and a_2^{2+} fragments versus the corresponding singly charged fragments formed by charge separation (b_2, a_2, and y_1) decreases in the Pro-His-Gly, Pro-His-Ala, and Pro-His-Leu series. A plausible explanation for this observation considers the increasing PA [27, 28] of the C-terminal fragment (G, A, and L for Pro-His-Gly, Pro-His-Ala, and Pro-His-Leu, respectively), which is likely to have a strong effect on the dissociation kinetics of the related s-DPD and as-DPD post-cleavage complexes. It is expected that as the PA of the C-terminal fragment increases formation of the doubly-charged b_2^{2+} ion becomes energetically less favorable.

Structure of [Pro−His-Gly + 2H]$^{2+}$

To understand atomic details of the fragmentation chemistry of doubly protonated Pro-His-Xaa, we have performed molecular dynamics and density functional theory calculations on doubly protonated Pro-His-Gly. In interpreting the experimental results, the first question concerns the sites of protonation in the [M + 2H]$^{2+}$ ions. The most likely sites would appear to be the imidazole ring of histidine and the N-terminal amine function. Bleiholder et al. [28] have shown that the imidazole side-chain of histidine has a proton affinity (232 kcal mol^{-1}) almost the same as the amine function of histidine while the proton affinity of imidazole itself (225.3 kcal mol^{-1}) [41] is quite high. Similarly, the proton affinity of proline (224 kcal mol^{-1}) [27, 28] also is quite high, making these the likely sites of protonation. Based on these considerations, we propose that the
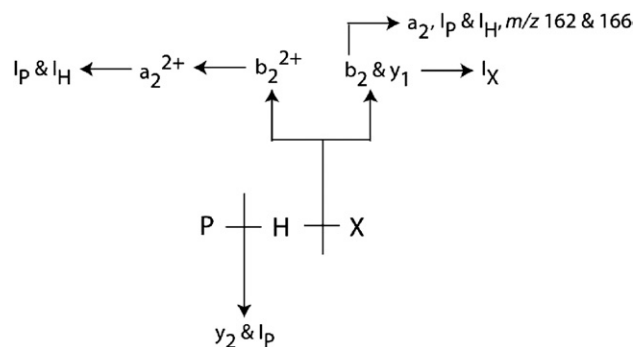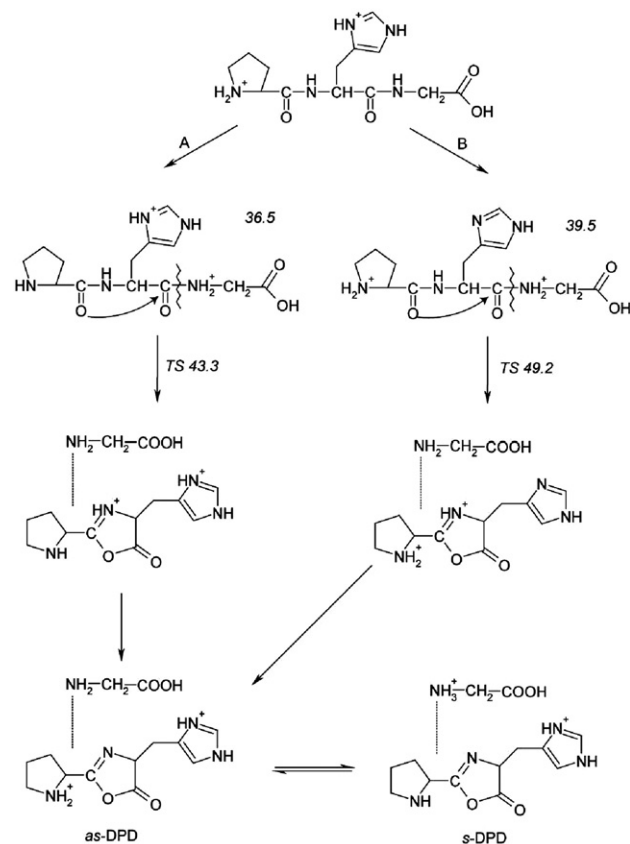

Scheme 2. Fragmentation pathways of doubly-protonated Pro-His-Xaa. For more details, see text.
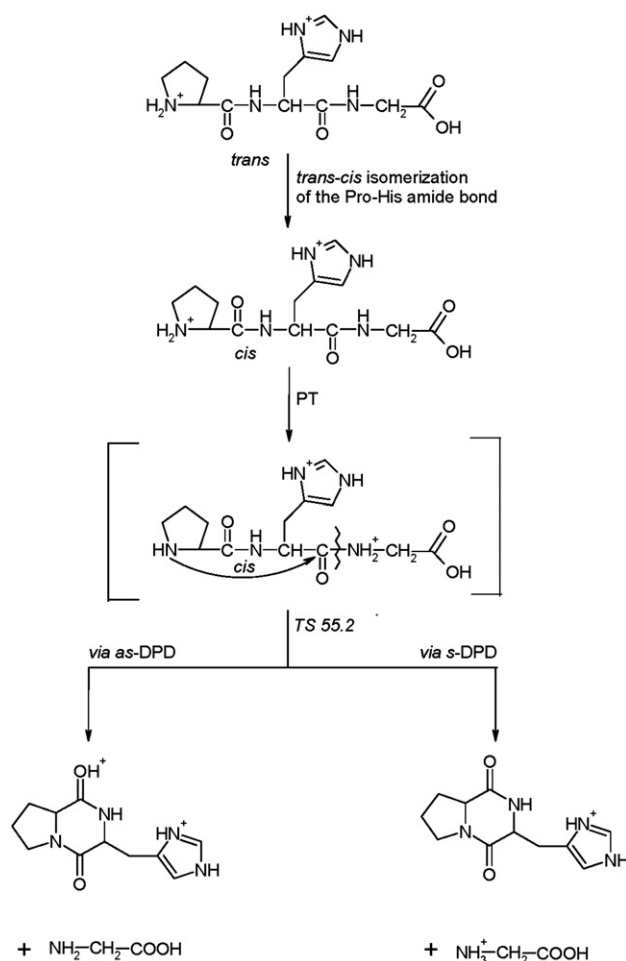
global minimum of $[M + 2H]^{2+}$ is a structure that is protonated at the N-terminus (Pro) and the His side chain. Two major forms were considered here, the *trans-trans* and *cis-trans* isomerization states of the backbone amide bonds (Structure A in Figure S1, and Structure A in Figure S2, Supplementary Material, which can be found in the electronic version of this article). The *trans-trans* structure is responsible for formation of oxazolone type *b* ions on the b_n-y_m pathways (Scheme 3, for more details, see below) [13, 31, 36, 42, 43]. On the other hand, the *cis-trans* isomer is necessary to form diketopiperazine isomers of *b* ions on the *cyclic-peptide* pathways (Scheme 4, for more details, see below) [13, 31, 44]. Our calculations (Table 1) indicate that the *trans-trans* form is ~8 kcal mol^{-1} more favored than the *cis-trans* structure. It is therefore likely that the doubly-charged parent ion is present in the mass spectrometer as the *all-trans* form.

Cleavage of the His-Gly Amide Bond on the b_2-y_1 (Oxazolone) Pathway

The first step on the oxazolone or b_n-y_m pathway (Scheme 3) is mobilization of a mobile proton to the His-Gly amide bond. This can be done by proton transfer from either the Pro amino group or from the
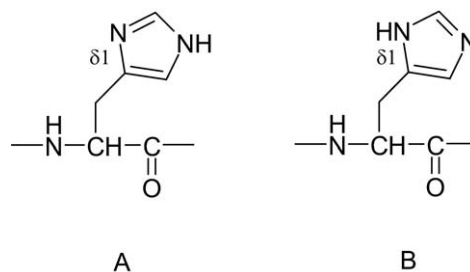

Scheme 4. Cleavage of the His-Gly amide bond on the *cyclic-peptide* pathway to form diketopiperazine isomer b_2 & b_2^{2+} and y_1 ions. Relative energies (kcal mol^{-1}) are indicated in italics.

His side chain. For the latter, one can consider two different tautomers of the neutral His side-chain (the $\delta1$ N either has a hydrogen or not):

Our calculations on various doubly-protonated Pro-His-Gly structures suggest that tautomer A is energetically much more favored therefore we do not consider form B in the following. This finding is in line with recent computational data by MacDonald and Thachuk [45] on protonated His-Gly.

The C-terminal amide nitrogen protonated structures of $[Pro-His-Gly + 2H]^{2+}$ with the second ionizing proton at the His side-chain or the N-terminus (Structures B and C in Figure S1) have similar relative

Scheme 3. Cleavage of the His-Gly amide bond on the b_2-y_1 pathway to form oxazolone isomer b_2 & b_2^{2+} and y_1 ions. Relative energies (kcal mol^{-1}) are indicated in italics.

Table 1. Total (E_{tot}, Hartree) and relative (E_{rel}, kcal mol^{-1}) energies and entropies (S, cal K^{-1} mol^{-1}) of the investigated species

					Doubly-protonated PHG			
Species	E_{tot}	E_{rel}	S		Species	E_{tot}	E_{rel}	S
NT and His protonation (*trans-trans*)	−1082.308807	0.0	156.8		NT and His protonation (*cis-trans*)	−1082.295935	8.4	154.5
NT and H-G amide N protonation	−1082.249868	36.5	153.9		His side-chain and H-G amide N protonation	−1082.243737	39.6	154.0
b_2-y_1 TS: NT protonation and neutral H	−1082.227263	49.2	151.9		b_2-y_1 TS: His side-chain protonation	−1082.236717	43.3	153.7
cyclic-peptide TS	−1082.219696	55.2	147.4		*His-b_2-y_1* reactive configuration	−1082.300709	5.3	155.9
His-b_2-y_1 TS	−1082.238873	43.8	152.4		*as*-DPD structure A	−1082.288863	11.3	163.4
as-DPD Structure B	−1082.280460	17.1	158.1		*s*-DPD charge separation TS b_2^{2+}	−1082.252426	34.7	n/a
A	−797.782056	0.0	120.0		B	−797.780403	1.6	123.6
C	−797.778944	2.6	122.8		D	−797.752791	17.7	122.8
E	−797.726579	34.3	121.1					

energies at 39.5 and 36.5 kcal mol^{-1} (Table 1), respectively. Note that the relative energies of these amide N protonated species are much higher than what is usually observed for single protonated peptides [13]. This is very likely due to the Coulomb repulsion of the two ionizing protons on this small peptide, which are forced to get closer to each other for the amide N protonated structures than for the global minimum. Cleavage of the C-terminal amide bond can be initiated from both structures (Paths A and B, Scheme 3) by nucleophilic attack of the Pro-His amide oxygen on the carbon center of the protonated amide bond. The b_2-y_1 TS (Scheme 3, Path A) with protonated His side-chain (43.3 kcal mol^{-1}, Structure D in Figure S1, Supplementary Material) is energetically clearly more favored than the one (Scheme 3, Path B) with neutral His side-chain (49.2 kcal mol^{-1}, second protonation at the N-terminus, Structure E in Figure S1, Supplementary Material). Our calculations indicate that the post-reaction doubly-protonated dimers (DPDs) formed right after crossing the two TSs are energetically not favored and undergo rapid intramolecular proton transfers (Scheme 3). On Path A, the extra proton on the just formed oxazolone ring transfers to the N-terminus of the b_2 ion. On Path B, the extra proton from the oxazolone nitrogen transfers to the His side-chain. These two proton transfer reactions lead to the same *as*-DPD (Scheme 3) with the ionizing protons located at the Pro amino and His side-chain moieties of the b_2^{2+} ion, respectively.

Figure 3 shows a few representative DPDs formed on the b_2-y_1 pathway. Structure A is the energetically most favored *as*-DPD at 11.3 kcal mol^{-1} relative energy. For this structure the two extra protons are efficiently solvated by intra- and intermolecular H-bonds leading to a surprisingly strongly-bonded doubly-charged post-reaction complex. It is worth noting here that no *s*-DPD can be formed from Structure A by a one-step proton transfer. This reaction is possible from Structure B, however (Figure 3), at 17.1 kcal mol^{-1} relative energy. Here, one of the extra protons is bridged in the

N_{Gly}...H-N$^+_{Pro}$ H-bond and intermolecular proton transfer results in an ion/ion complex where both monomers are charged. The dissociation energetics of this complex has been studied in constrained optimizations where the distance of H and N_{Pro} was kept fixed at predefined values (1.5–6.0 Å, 0.5 Å steps) and all other molecular parameters were fully optimized. These calculations give a curve with a maximum at 4 Å, and the corresponding structure is shown in Figure 3. The relative energy of this charge separation TS is 34.7 kcal mol^{-1}, which is lower than that of the b_2-y_1 amide bond cleavage TS (43.3 kcal mol^{-1}). It is worth noting here that the charge separation TS shown in Figure 3 as Structure C is one of the many possible such TSs for doubly-protonated Pro-His-Gly, so its energy should be
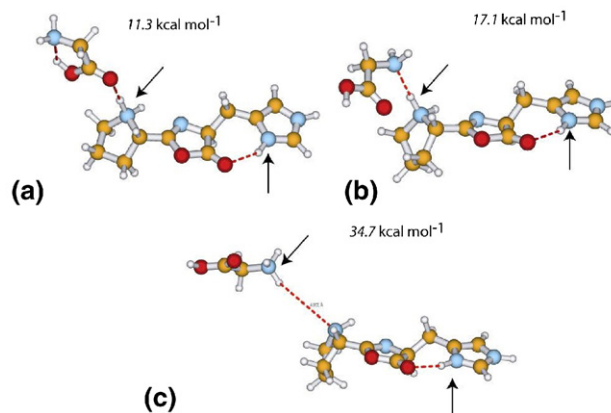

Figure 3. Post-reaction doubly-protonated dimers (DPDs) on the b_2-y_1 pathway: (**a**) energetically most favored *as*-DPD with protonation at the Pro amino and His side-chain moieties, (**b**) a higher energy *as*-DPD where PT to Gly is possible, (**c**) charge separation transition structure. Ionizing protons are denoted by arrows and relative energies are given in italics.

considered only as an approximation (upper bound) to the true threshold energy of the charge separation process.

The dissociation energetics of *as*-DPD and *s*-DPD are rather different. The former dissociates in a barrier-less endothermic process to form the oxazolone isomer of b_2^{2+} (for more details on this isomer *vide infra*) and Gly at 44.6 kcal mol^{-1} relative energy (Table 1). On the other hand, *s*-DPD dissociate to form separated b_2 and y_1 ions at 3.7 kcal mol^{-1} relative energy. These energetics suggest that no b_2^{2+} ions are formed upon CID of doubly-protonated Pro-His-Gly, and only the singly charged b_2 and y_1 fragments will be detected. As the product ion spectrum displayed in Figure 1 shows this is not the case: b_2^{2+} is as abundant as b_2 and a_2^{2+} (formed from b_2^{2+}) is more abundant than a_2. Formation of the doubly-charged fragments can be explained by the substantial charge separation barrier (TS approximately at 35 kcal mol^{-1} relative energy) observed for the dissociation of *s*-DPD.

Formation of Diketopiperazine b_2^{2+} Isomers on the Cyclic-Peptide Pathway

The first step on the *cyclic-peptide* pathway is *trans* to *cis* isomerization of the Pro-His amide bond. This involves species where the His amide nitrogen is protonated, reducing the partial double-bond character of the Pro-His amide bond to allow rotation [44]. As described above, the resulting Pro nitrogen and His side-chain protonated *cis-trans* form (Structure A in Figure S2, Supplementary Material) is energetically less favored than the *trans-trans* structures by ~8 kcal mol^{-1}. In the next step, the ionizing proton from the Pro nitrogen is transferred to the His-Gly amide nitrogen, followed by nucleophilic attack of the Pro nitrogen on the carbon center of the protonated His-Gly amide bond. Our calculations indicate that the proton transfer and nucleophilic attack occur in a concerted manner. While we could locate some high-energy His-Pro amide nitrogen protonated structures as local minima, most of these structures undergo spontaneous proton transfer to the Pro nitrogen during the course of geometry optimizations. This behavior is noted in Scheme 4 by putting the respective structure into parentheses. The energetically most favored TS (Structure B in Figure S2, Supplementary Material) we located in our scans is at 55.2 kcal mol^{-1} relative energy, which is much higher than the threshold energy of the b_2-y_1 pathway (43.3 kcal mol^{-1}). Furthermore, the reaction entropies (ΔS_{298}, −3.1, and −9.8 cal mol^{-1} K^{-1} (Table 1) for the b_2-y_1 and cyclic-peptide pathways, respectively) clearly disfavor formation of diketopiperazine b_2^{2+} isomers. These energetics and entropy effects indicate that the cyclic-peptide pathway is not active for doubly-protonated Pro-His-Gly.

His Side-Chain Initiated Amide Bond Cleavage: Formation of b_2 Isomers with Fused Imidazole and Lactam Rings

The amide bond cleavage pathway initiated by the His side-chain (referred to as His-b_n-y_m) was studied in detail by Wysocki, O'Hair, and coworkers [11, 25, 26]. Based on these investigations, we proposed a mechanism that involves transfer of the extra ionizing proton from the His side-chain to the C-terminal adjacent amide nitrogen and subsequent nucleophilic attack of the imidazole nitrogen on the carbon of the protonated amide bond [13]. Our calculations on doubly-protonated Pro-His-Gly indicate that transfer of the ionizing proton and nucleophilic attack by the His side-chain occur in a concerted manner. The corresponding TS (Scheme 5; Structure B in Figure S3, Supplementary Material) has a low threshold energy at 43.8 kcal mol^{-1}. On the reactant wing of this TS no stable amide N protonated structure was found by IRC calculations. Instead, the extra proton on the amide N transfers back to the His side-chain, and the related structure is stabilized in a H-bond with the C-terminal COOH group (5.3 kcal mol^{-1} relative energy, Structure A in Figure S3). In other words, the His pathway can be initiated by "local" proton transfer from protonated His side-chain, and the related structures are usually energetically more favored than amide nitrogen protonated structures, which are reactive configurations on the b_n-y_m pathways. The reaction entropy of the His-b_2-y_1 channel [−4.4 cal mol^{-1} K^{-1} (Table 1)] is similar to that of the oxazolone b_2-y_1 pathway (−3.1 cal mol^{-1} K^{-1}). The similar threshold energies and reaction entropies obtained for the oxazolone b_2-y_1 and His-b_2-y_1 channels suggest the b_2^{2+} population contains both oxazolone and fused ring isomers. However, the accuracy of the
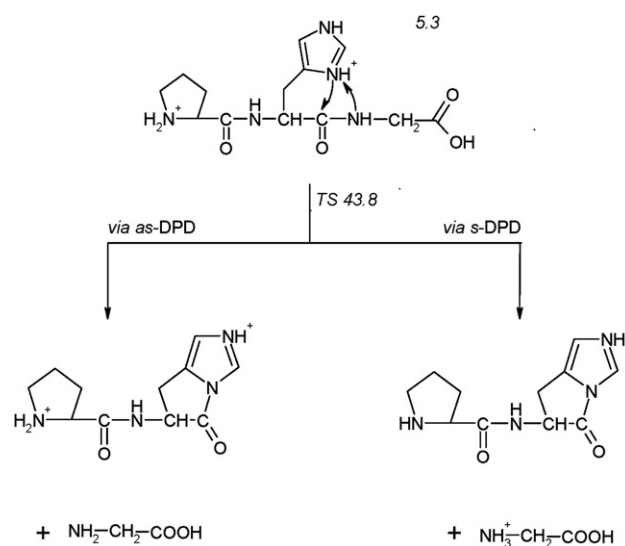
Scheme 5. Cleavage of the His-Gly amide bond on the His-b_n-y_m pathway to form b_2 & b_2^{2+} and y_1 ions. The b_2^{2+} and b_2 ions have fused imidazole and lactam rings at their C-terminus. Relative energies (kcal mol^{-1}) are indicated in italics.
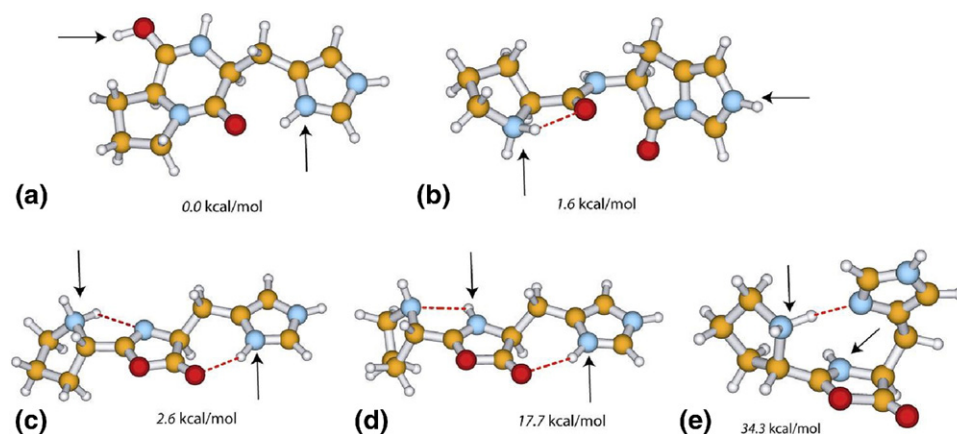
Figure 4. Various b_2^{2+} structures derived for the sequence Pro-His. Relative energies are denoted in italics and ionizing protons are denoted by arrows. (a) Diketopiperazine (b) fused ring and (c-e) oxazolone isomer b_2^{2+} structures derived for the sequence Pro-His. Relative energies are denoted in italics and ionizing protons are denoted by arrows.

applied theoretical models does not allow more quantitative estimation of the relative weight of the two isomers.

Structural Isomers of b_2^{2+} Ions

The threshold energies of the b_n-y_m, cyclic-peptide, and His-b_n-y_m amide bond cleavage pathways are at 43.3, 55.2, and 43.8 kcal mol^{-1}, respectively, while the corresponding reaction entropies are -3.1, -9.8, and -4.4 cal mol^{-1} K^{-1} (Table 1). This energetics indicates that the b_2^{2+} ion population will be dominated by the oxazolone and fused ring isomers with very minor diketopiperazine forms if the various b_2^{2+} isomers do not interconvert after their formation. Our calculations on the b_2^{2+} isomers indicate that the energetically most favored form is the diketopiperazine isomer (Figure 4, Structure A), which is stabilized by a strong $N_{\delta 1}$–H. . .O H-bond. The fused ring b_2^{2+} isomer (Figure 4, Structure B) formed on the His-b_n-y_m pathway is at 1.6 kcal mol^{-1} relative energy, while the energetically most favored oxazolone structure (Figure 4, Structure C) with protonation at the Pro nitrogen and His side-chain is at 2.6 kcal mol^{-1} relative energy. It is worth noting that a few other protonated forms are possible for the oxazolone structure. For example, proton transfer from the Pro nitrogen to the oxazolone ring leads to a structure (Figure 4, Structure D) at 17.7 kcal mol^{-1} relative energy. Furthermore, proton transfer from the His side-chain to the oxazolone ring results in a structure (Figure 4, Structure E) at more than 30 kcal mol^{-1} relative energy. This structure is very likely involved in re-isomerization pathways between the oxazolone and fused-ring b_2^{2+} structures, since nucleophilic attack of the imidazole $N_{\delta 1}$ on the carbonyl C of the oxazolone ring leads to the fused-ring isomer. Since structure E is energetically less favored, we propose that these structures do not interconvert to one another due to the high-energy intermediates involved.

Conclusions

Electrospray ionization from acidic solutions of tripeptides with histidine in the central position results in significant yields of doubly-protonated ions [M + 2H]$^{2+}$. This affords the opportunity to study the fragmentation reactions of relatively simple doubly-charged species. When proline is in the N-terminal position as in Pro-His-Xaa (Xaa = Gly, Ala, Leu) fragmentation results, in part, in the formation of b_2^{2+} ions; such small doubly-charged b ions have not been observed previously upon CID of small doubly-protonated peptides, although a brief mention [23] has been made of the formation of a b_2^{2+} ion from doubly-protonated Substance P. However, the main fragmentation reactions observed remain charge separation reactions producing b_2 and y_2 ions at higher mass.

Our calculations on doubly-protonated Pro-His-Gly indicate that the energetically most favored structure on the PES is a *trans-trans* species with protonations at the Pro nitrogen and His side-chain. Cleavage of the His-Gly amide bond is possibly involves TSs at 43–44 kcal mol^{-1} relative energies on the b_n-y_m and His-b_n-y_m pathways to form b_2^{2+} and b_2 ions with oxazolone and fused imidazole and lactam rings, respectively. These channels are both energetically and entropically more favored than the *cyclic-peptide* pathway that leads to diketopiperazine derivative b_2 isomers. Limited scans of the doubly-protonated post-cleavage complexes on the b_2-y_1 pathway indicate that charge-separation to form b_2 and y_1 ions involves a significant barrier. Further work will explore the prevalence of doubly-protonated species in small peptides containing basic residues and delineate their fragmentation modes.

Acknowledgments

Appendix A
Supplementary Material

Supplementary material associated with this article may be found in the online version at doi:10.1016/j.jasms.2009.07.002.

References

 1. Whitehouse, C. M.; Dreyer, R. N.; Yamashita, M.; Fenn, J. B. Electrospray Interface for Liquid Chromatographs and Mass Spectrometers. *Anal. Chem.* **1985,** *57,* 675–679.
 2. Cole, R. B, Ed. *Electrospray Ionization Mass Spectrometry. Fundamentals, Instrumentation, and Applications*; Wiley: New York, 1997; p. 577.
 3. Pramanik, B. N.; Ganguly, A. K.; Gross, M. L., Eds. *Applied Electrospray Mass Spectrometry*; Marcel Dekker: New York, 2002; p. 434.
 4. Karas, M.; Hillenkamp, F. Laser Desorption Ionization of Proteins with Molecular Masses Exceeding 10,000 Daltons. *Anal. Chem.* **1988,** *60,* 2299–2301.
 5. Beavis, R. C.; Chait, B. T. Matrix-Assisted Laser Desorption Ionization Mass-Spectrometry of Proteins. *Methods Enzymol.* **1996,** *270,* 519–551.
 6. McLafferty, F. W., Ed.; Tandem Mass Spectrometry; Wiley: New York, 1983; p. 506.
 7. Busch, K. L.; Glish, G. L.; McLuckey, S. A. Mass Spectrometry/Mass Spectrometry: Techniques and Applications of Tandem Mass Spectrometry. VCH: New York, 1988; p. 443.
 8. O'Hair, R. A. J. Commentary—The Role of Nucleophile–Electrophile Interactions in the Unimolecular and Bimolecular Gas-Phase Ion Chemistry of Peptides and Related Systems. *J. Mass Spectrom.* **2000,** *35,* 1377–1381.
 9. Schlosser, A.; Lehmann, W. D. Commentary—Five-Membered Ring Formation in Unimolecular Reactions of Peptides: A Key Structural Element Controlling Low-Energy Collision-Induced Dissociation of Peptides. *J. Mass Spectrom.* **2000,** *35,* 1382–1390.
10. Polce, M. J.; Ren, D.; Wesdemiotis, C. Commentary—Dissociation of the Peptide Bond in Protonated Peptides. *J. Mass Spectrom.* **2000,** *35,* 1391–1398.
11. Wysocki, V. H.; Tsaprailis, G.; Smith, L. L.; Breci, L. A. Commentary—Mobile and Localized Protons: A Framework for Understanding Peptide Dissociation. *J. Mass Spectrom.* **2000,** *35,* 1399–1406.
12. Vaisar, T. In *Encyclopedia of Mass Spectrometry*, Vol. IV., Nibbering, N.M.M., Ed.; Elsevier: New York, 2005; p. 752.
13. Paizs, B.; Suhai, S. Fragmentation Pathways of Protonated Peptides. *Mass Spectrom. Rev.* **2005,** *24,* 508–548.
14. Tang, X.-J.; Boyd, R. K. An Investigation of Fragmentation Mechanisms of Doubly-Protonated Tryptic Peptides. *Rapid Commun. Mass Spectrom.* **1992,** *6,* 651–657.
15. Tang, X.-J.; Thibault, P.; Boyd, R. K. Fragmentation Reactions of Multiply-Protonated Peptides and Implications for Sequencing by Tandem Mass Spectrometry with Low-Energy Collision-Induced Dissociation. *Anal. Chem.* **1993,** *65,* 2824–2834.
16. Tang, X.-J.; Boyd, R. K. Rearrangements of Doubly Charged Acylium Ions from Lysyl and Ornithyl Peptides. *Rapid Commun. Mass Spectrom.* **1994,** *8,* 678–686.
17. Tsaprailis, G.; Nair, H.; Zhong, W.; Kuppannan, K.; Futrell, J. H.; Wysocki, V. H. A Mechanistic Investigation of the Enhanced Cleavage at Histidine in the Gas-Phase Dissociation of Protonated Peptides. *Anal. Chem.* **2004,** *76,* 2083–2094.
18. Tabb, D. L.; Smith, L. L.; Breci, L. A.; Wysocki, V. H.; Lin, D.; Yates JR III. Statistical Characterization of Ion Trap Tandem Mass Spectra from Doubly-Charged Tryptic Peptides. *Anal. Chem.* **2003,** *75,* 1155–1163.
19. Kapp, E. A.; Schütz, F.; Reid, G. E.; Eddes, J. S.; Moritz, R. L.; O'Hair, R. A. J.; Speed, T. P.; Simpson, R. J. Mining a Tandem Mass Spectrometry Database to Determine the Trends and Global Factors Influencing Peptide Fragmentation. *Anal. Chem.* **2003,** *75,* 6251–6264.
20. Zhang, Z. Prediction of Low-Energy Collision-Induced Dissociation Spectra of Peptides. *Anal. Chem.* **2004,** *76,* 3908–3922.
21. Bleiholder, C.; Suhai, S.; Somogyi, A.; Paizs, B. Fragmentation Pathways of Doubly Protonated Tryptic Peptides. *J. Am. Soc. Mass Spectrom.,* unpublished.
22. Haselmann, K. F.; Budnik, B. A.; Zubarev, R. A. Electron Capture Dissociation of b(2+) Peptide Fragments Reveals the Presence of the Acylium Ion Structure. *Rapid Commun. Mass Spectrom.* **2000,** *14,* 2242–2246.
23. Quin, X.-Z.; Yuan, Y. Electrospray Ionization/Collision-Induced Dissociation of Protonated Substance P Ions—Effect of Charge on the Fragmentation Patterns. *Int. J. Mass Spectrom.* **2004,** *237,* 123–133.
24. Shi, T.; Siu, C. K.; Siu, K. W. M.; Hopkinson, A. C. Di-positively Charged Protonated a_3 and a_2 Ions: Generation by Fragmentation of [La(GGG)(CH$_3$CN)$_2$]$^{3+}$. *Angew. Chem. Int. Ed.* **2008,** *47,* 8288–8291.
25. Farrugia, J. M.; Taverner, T.; O'Hair, R. A. J. Side-chain Involvement in the Fragmentation Reactions of the Protonated Methyl Esters of Histidine and Its Peptides. *Int. J. Mass Spectrom.* **2001,** *209,* 99–112.
26. Farrugia, J. M.; O'Hair, R. A. J.; Reid, G. E. Do All b_2 Ions Have Oxazolone Structures? Multistage Mass Spectrometry and Ab Initio Studies on Protonated N-Acyl Amino Acid Methyl Ester Model Systems. *Int. J. Mass Spectrom.* **2001,** *210/211,* 71–87.
27. Harrison, A. G. The Gas-Phase Basicities and Proton Affinities of Amino Acids and Peptides. *Mass Spectrom. Rev.* **1997,** *16,* 201–217.
28. Bleiholder, C.; Suhai, S.; Paizs, B. Revising the Proton Affinity Scale of the Naturally Occurring □-Amino Acids. *J. Am. Soc. Mass Spectrom.* **2006,** *17,* 1275–1281.
29. Wyttenbach, T; Paizs, B.; Barran, P.; Breci, L.; Liu, D.; Suhai, S.; Wysocki, V. H.; Bowers, M. T. The Effect of the Initial Water of Hydration on the Energetics, Structures, and H/D-exchange Mechanism of a Family of Pentapeptides: An Experimental and Theoretical Study. *J. Am. Chem. Soc.* **2003,** *125,* 13768–13775.
30. Polfer, N. C.; Oomens, J.; Suhai, S.; Paizs, B. Infrared Spectroscopy and Theoretical Studies on Gas-Phase Protonated Leu-Enkephalin and Its Fragments: Direct Experimental Evidence for the Mobile Proton. *J. Am. Chem. Soc.* **2007,** *129,* 5887–5897.
31. Paizs, B.; Suhai, S. Towards Understanding the Tandem Mass Spectra of Protonated Oligopeptides. I. Mechanism of Amide Bond Cleavage. *J. Am. Soc. Mass Spectrom.* **2004,** *15,* 103–112.
32. Paizs, B.; Suhai, S.; Hargittai, B.; Hruby, V. J.; Somogyi, A. Ab Initio and MS/MS Studies on Protonated Peptides Containing Basic and Acidic Amino Acid Residues. I. Solvated Proton Versus Salt-Bridged Structures and the Cleavage of the Terminal Amide Bond of Protonated RD-NH$_2$. *Int. J. Mass Spectrom.* **2002,** *219,* 203–232.
33. Bleiholder, C.; Osburn, S.; Williams, T. D.; Suhai, S.; Van Stipdonk, M.; Harrison, A. G.; Paizs, B. Sequence Scrambling Fragmentation Pathways of Protonated Peptides. *J. Am. Chem. Soc.* **2008,** *130,* 17774–17789.
34. Bythell, B. J.; Somogyi, Á.; Paizs, B. What is the Structure of b_2 Ions Generated from Doubly Protonated Tryptic Peptides? *J. Am. Soc. Mass Spectrom.* **2009,** *20,* 618–624.
35. Case, D. A.; Pearlman, D. A.; Caldwell, J. W.; Cheatham III, T. E.; Ross, W. S.; Simmerling, C. L.; Darden, T. A.; Merz, K. M.; Stanton, R. V.; Cheng, A. L.; Vincent, J. J.; Crowley, M.; Tsui, V.; Radmer, R. J.; Duan, Y.; Pitera, J.; Massova, I. G.; Seibel, G. L.; Singh, U. C.; Weiner, P. K.; Kollmann, P. A. AMBER 99, University of California: San Francisco.
36. Paizs, B.; Suhai, S. Combined Quantum Chemical and RRKM Modeling of the Main Fragmentation Pathways of Protonated GGG. II. Formation of b_2, y_1, and y_2 ions. *Rapid Commun. Mass Spectrom.* **2002,** *16,* 375–389.
37. Frisch, M. J.; Trucks, G. W.; Schlegel, H. B.; Scuseria, G. E.; Robb, M. A.; Cheeseman, J. R.; Zakrzewski, V. G.; Montgomery, J. A. J.; Stratman, R. E.; Burant, J. C.; Dapprich, S.; Millam, J. M.; Daniels, A. D.; Kudin, A. N.; Strain, M. C.; Farkas, O.; Tomasi, J.; Barone, V.; Cossi, M.; Cammi, R.; Mennucci, B.; Pomelli, C.; Adamo, C.; Clifford, S.; Ochterski, J.; Petersson, G. A.; Ayala, P. Y.; Cui, Q.; Morokuma, K.; Malick, D. K.; Rabuck, A. D.; Raghavachari, K.; Foresman, J. B.; Cioslowski, J.; Ortiz, J. V.; Stefanov, B. B.; Liu, G.; Liashenko, A.; Piskorz, P.; Komaromi, I.; Gombertz, R.; Martin, R. L.; Fox, D. J.; Keith, T.; Al-Laham, M. A.; Peng, C. Y.; Nanyakkara, A.; Gonzalez, C.; Challacombe, M.; Gill, P. M. W.; Johnsen, B. G.; Chen, W.; Wong, M. W.; Andres, J. L.; Head-Gordon, M.; Replogle, E. S.; Pople, J. A. *Gaussian 03, Revision C. 02,* Gaussian Inc.: Pittsburgh, PA.
38. Harrison, A. G.; Young, A. B.; Schnölzer, M.; Paizs, B. Formation of Iminium Ions by Fragmentation of a_2 Ions, *Rapid Commun. Mass Spectrom.* **2004,** *18,* 1635–1640.
39. Tsang, C. W.; Harrison, A. G. Chemical Ionization of Amino Acids. *J. Am. Chem. Soc.* **1976,** *98,* 1301–1308.
40. Dookeran, N. N.; Talcin, T.; Harrison, A. G. Fragmentation Reactions of Protonated α-Amino Acids. *J. Mass Spectrom.* **1996,** *31,* 500–508.
41. Hunter, E. P.; Lias, S. G. Evaluated Gas Phase Basicities and Proton Affinities of Molecules: An Update. *J. Phys. Chem. Ref. Data* **1998,** *27,* 413–656.
42. Yalcin, T.; Csizmadia, I. G.; Peterson, M. R.; Harrison, A. G. The Structure and Fragmentation of b_n ($n \geq 3$) Ions in Peptide Spectra. *J. Am. Soc. Mass Spectrom.* **1996,** *7,* 233–242.
43. Yalcin, T.; Khouw, C.; Csizmadia, I. G.; Peterson, M. R.; Harrison, A. G. Why Are b Ions Stable Species in Peptide Spectra? *J. Am. Soc. Mass Spectrom.* **1995,** *6,* 1165–1174.
44. Paizs, B.; Suhai, S. Combined Quantum Chemical and RRKM Modeling of the Main Fragmentation Pathways of Protonated GGG. I. *Cis-trans* Isomerization Around Protonated Amide Bonds. *Rapid Commun. Mass Spectrom.* **2002,** *15,* 2307–2323.
45. MacDonald, B. I.; Thachuk, M. Gas-Phase Proton Transfer Pathways in Protonated Histidylglycine. *Rapid Commun. Mass Spectrom.* **2008,** *22,* 2946–2954.